

# CONVOLUTIONAL GENERATIVE ADVERSARIAL NETWORKS WITH BINARY NEURONS FOR POLYPHONIC MUSIC GENERATION

Hao-Wen Dong and Yi-Hsuan Yang

Research Center for IT Innovation, Academia Sinica  
{salu133445, yang}@citi.sinica.edu.tw

## ABSTRACT

It has been shown recently that convolutional generative adversarial networks (GANs) are able to capture the temporal-pitch patterns in music using the piano-roll representation, which represents music by binary-valued time-pitch matrices. However, existing models can only generate real-valued piano-rolls and require further post-processing (e.g. hard thresholding, Bernoulli sampling) at test time to obtain the final binary-valued results. In this work, we first investigate how the real-valued predictions generated by the generator may lead to difficulties in training the discriminator. To overcome the binarization issue, we propose to append to the generator an additional refiner network, which uses binary neurons at the output layer. The whole network can be trained in a two-stage training setting: the generator and the discriminator are pre-trained in the first stage; the refiner network is then trained along with the discriminator in the second stage to refine the real-valued piano-rolls generated by the pretrained generator to binary-valued ones. The proposed model is able to directly generate binary-valued piano-rolls at test time. Experimental results show improvements to the existing models in most of the evaluation metrics. All source code, training data and audio samples can be found at <https://salu133445.github.io/bmusegan/>.

## 1. INTRODUCTION

Recent years have seen increasing research on symbolic-domain music generation and composition using deep neural networks [6]. Notable progress has been made to generate monophonic melodies [25,28], lead sheets (i.e., melody and chords) [7, 10, 27], or four-part chorales [14]. To add something new to the table and to increase the polyphony and number of instruments of the generated music, we study in this paper the generation of music in a more general yet less studied (in recent work on music generation) representation known as the piano-roll representation. As Figure 1 shows, we can consider an  $M$ -track piano-roll as a collection of  $M$  binary-valued time-pitch matrices indicating the presence of pitches per time step for each track.

Generating piano-rolls is challenging because of the large number of possible active notes per time step and the involvement of multiple instruments. Unlike a melody or a chord progression, which can be viewed as a sequence of note/chord events and modeled by a recurrent neural network (RNN) [21,24], the musical texture in a piano-roll is

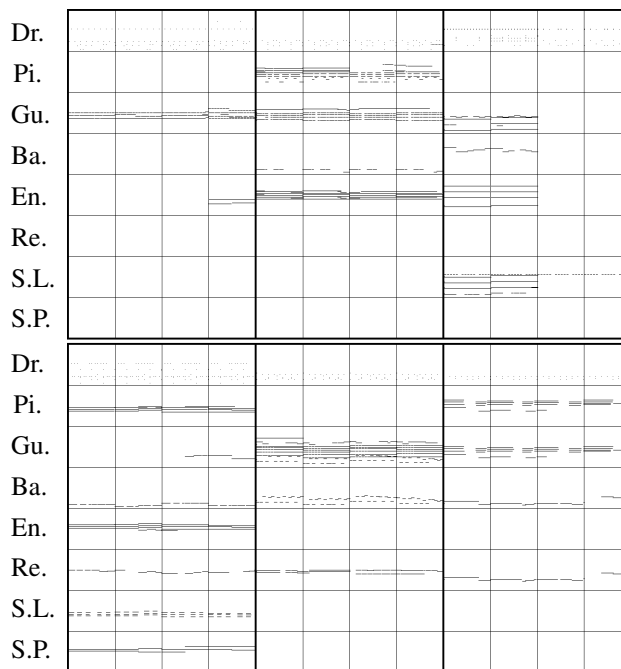


**Figure 1.** Six examples of eight-track piano-roll of four-bar long (each block represents a bar) seen in our training data. The eight tracks are *Drums, Piano, Guitar, Bass, Ensemble, Reed, Synth Lead* and *Synth Pad*.

much more complex (see Figure 1). While RNNs may be good at learning the temporal dependency of music, convolutional neural networks (CNNs) are usually considered better at learning local patterns [18].

For this reason, in our previous work [9], we used a convolutional generative adversarial network (GAN) [11] to generate five-track piano-rolls and showed that the model is able to produce something exhibiting drum patterns and plausible note events. However, musically the generated result is still far from satisfying to human ears, scoring around 3 on average on a five-level Likert scale in overall quality in the reported user study.<sup>1</sup>

There are several ways to improve upon this prior work. The major topic we are interested in is the introduction of *binary neurons* (BNs) [1, 3] to the model. We note that conventional CNN designs, also the one adopted in our

<sup>1</sup> Another related work on generating piano-rolls, as presented by Boulanger-Lewandowski *et al.* [5], replaced the output layer of an RNN with conditional restricted Boltzmann machines (RBMs) to model high-dimensional sequences and applied the model to generate piano-rolls sequentially (i.e. one time step after another).

previous work [9], can only generate real-valued predictions and require further postprocessing (e.g., hard thresholding or Bernoulli sampling) at test time to obtain the final binary-valued piano-rolls.<sup>2</sup> This raises two issues.

- First, naïve methods for binarizing a piano-roll can easily lead to overly-fragmented notes. This happens when the generated real-valued piano-roll has many entries with values close to the threshold in the case of hard thresholding. For Bernoulli sampling, a time-pitch point would take the value 1 with probability equal to the value of the corresponding entry in the real-valued piano-roll. Due to the stochastic nature, it is possible to fire a note even for an entry with low probability.
- Second, the real-valued predictions generated by the generator  $G$  in GAN may lead to difficulties in training the discriminator counterpart  $D$  (see Section 2.1 for a brief introduction of GAN). Using real-valued instead of binary-valued inputs increases the model space from  $2^N$  to  $\mathbb{R}^N$ , where  $N$  is the product of the number of time steps and the number of possible pitches, requiring  $D$  to learn the decision boundaries in discriminating real from generated music in a substantially larger space, as Figure 2 illustrates. Moreover, after passing through the first few convolutional layers of  $D$ , a real-valued piano-roll generated by  $G$  may look similar to a binary-valued piano-roll sampled from real data. As a result,  $G$  does not need to “learn hard” to generate realistic result for it already has a shortcut to create the so-called *adversarial examples* [12, 26] to fool  $D$ .<sup>3</sup>

The use of BNs can mitigate these issues, since the binarization is part of the training process and the input to  $D$  is always binary-valued piano-rolls. We propose to achieve so by appending to the end of  $G$  an additional *refiner network*  $R$  that uses either deterministic BNs (DBNs) or stochastic BNs (SBNs) at the output layer. In this way,  $G$  produces real-valued predictions and  $R$  refines them into binary ones. We train the whole network in a two-stage training setting:  $G$  and  $D$  are pretrained in the first stage;  $R$  is then trained along with  $D$  in the second stage.

The proposed model is able to directly generate binary-valued piano-rolls at test time. We examine and compare different binarization strategies and different training strategies. Experimental results show improvements to the existing models in most of the evaluation metrics and demonstrate the effectiveness of two-stage training strategy. Finally, a user study of 20 subjects shows a preference to DBNs for the proposed model.

All source code, training data and audio samples can be found on our project website.<sup>4</sup>

<sup>2</sup> Such binarization is typically not needed for an RNN or an RBM in polyphony music generation, since an RNN is usually used to predict predefined note events [22] and an RBM is often used with binary visible and hidden units and sampled by Gibbs sampling [5, 20].

<sup>3</sup> In other words, a generated real-valued piano-roll, obviously not a real one to human eyes for it is not binary, may be classified as real by  $D$ .

<sup>4</sup> <https://salu133445.github.io/bmusegan/>

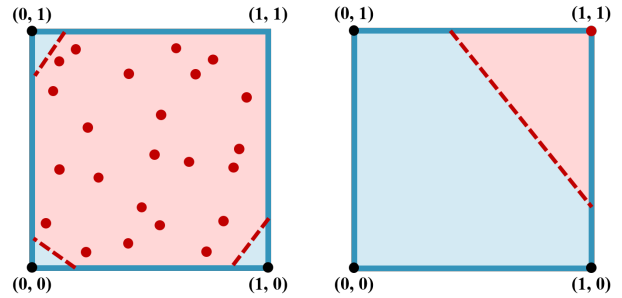


**Figure 2.** An illustration of the decision boundaries (red dashed lines) that the discriminator  $D$  has to learn when the generator  $G$  outputs (left) real values and (right) binary values. The decision boundaries divide the space into the *real* class (in blue) and the *fake* class (in red). The black and red dots represent the real data and the fake ones generated by the generator, respectively. We can see that the decision boundaries are easier to learn when the generator outputs binary values rather than real values.

## 2. BACKGROUND

### 2.1 Generative Adversarial Networks

A generative adversarial network (GAN) [11] has two core components: a *generator*  $G$  and a *discriminator*  $D$ . The former takes as input a random vector  $\mathbf{z}$  sampled from a prior distribution  $p_z$  and generates a fake data  $G(\mathbf{z})$ .  $D$  takes as inputs either real data  $\mathbf{x}$  or fake data generated by  $G$ . During training time,  $D$  learns to distinguish fake data from real ones, whereas  $G$  learns to fool  $D$ .

It has been found that using the Wasserstein distance instead of Jensen-Shannon divergence as the cost function in GAN can lead to better generation result [9]. Comparing to ordinary GANs, the Wasserstein GAN (WGAN) [2] has a more stable training process and it can better deal with the so-called mode collapse issue [11]. The objective functions for WGAN can be formulated as:

$$\min_G \max_D \mathbf{E}_{\mathbf{x} \sim p_d} [D(\mathbf{x})] - \mathbf{E}_{\mathbf{z} \sim p_z} [D(G(\mathbf{z}))], \quad (1)$$

where  $p_d$  denotes the real data distribution. Gulrajani *et al.* later proposed to add to the objective function of  $D$  a *gradient penalty* (GP) term [13]:  $\mathbf{E}_{\hat{\mathbf{x}} \sim p_{\hat{\mathbf{x}}}} [(\|\nabla_{\hat{\mathbf{x}}} D(\hat{\mathbf{x}})\| - 1)^2]$ , where  $p_{\hat{\mathbf{x}}}$  is defined sampling uniformly along straight lines between pairs of points sampled from  $p_d$  and  $p_g$ , the model distribution. Empirically they found it speed up the training compared to the weight clipping strategy used in the original WGAN. Hence, we choose WGAN-GP as our generative framework.

### 2.2 Stochastic and Deterministic Binary Neurons

Binary neurons (BNs) are neurons that output binary-valued predictions. In this work, we consider two types of BNs: deterministic binary neurons (DBNs) and stochastic binary neurons (SBNs). DBNs act like neurons with *hard thresholding* functions as their activation functions. We define the output of a DBN for a real-valued input  $x$  as:

$$DBN(x) = \mathbf{1}_{\sigma(x) > 0.5}, \quad (2)$$

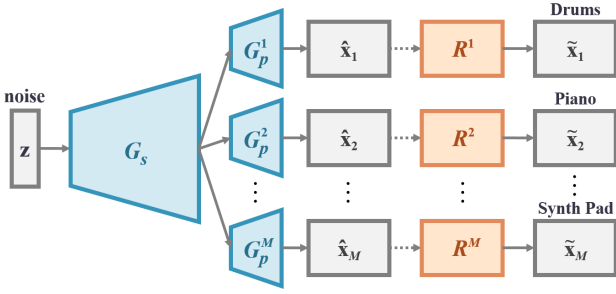


**Figure 3.** The generator and the refiner. The generator produces real-valued predictions. The refiner network refines the outputs of the generator into binary ones.



**Figure 4.** The refiner network. The tensor size remains the same throughout the network.

where  $\mathbf{1}_{(\cdot)}$  is the indicator function and  $\sigma(\cdot)$  is the logistic sigmoid function. SBNs, in contrast, binarize an input  $x$  according to a probability, defined as:

$$SBN(x) = \mathbf{1}_{z < \sigma(x)}, \quad z \sim U[0, 1], \quad (3)$$

where  $U[0, 1]$  denotes a uniform distribution.

### 2.3 Straight-through Estimator

Computing the exact gradients for either DBNs or SBNs, however, is intractable, for doing so requires the computation of the average loss over all possible binary samplings of all the BNs, which is exponential in the total number of BNs. As a result, the flow of backpropagation used to train parameters of the network would be blocked.

A few solutions have been proposed to address this issue [1, 3]. One strategy is to replace the non-differentiable functions, which are used in the forward pass, by differentiable functions (usually called the *estimators*) in the backward pass. We adopt the *straight-through* (ST) estimator proposed by Hinton [17] in this work. In the backward pass, ST simply treats BNs as identity functions and ignores their gradients. This leads to some biases but it works empirically. A variant is the sigmoid-adjusted ST estimator, which multiply the gradients in the backward pass by the derivative of the sigmoid function. The latter was successfully employed in training sophisticated networks [8]. Accordingly, we resort to the sigmoid-adjusted ST estimator when training networks with DBNs and SBNs.

## 3. PROPOSED MODEL

### 3.1 Data Representation

Following [9], we use the multi-track piano-roll representation. A multi-track piano-roll is defined as a set of piano-rolls for different tracks or instruments. Each piano-roll is a binary-valued score-like matrix, where its vertical and horizontal axis represent note pitch and time, respectively.

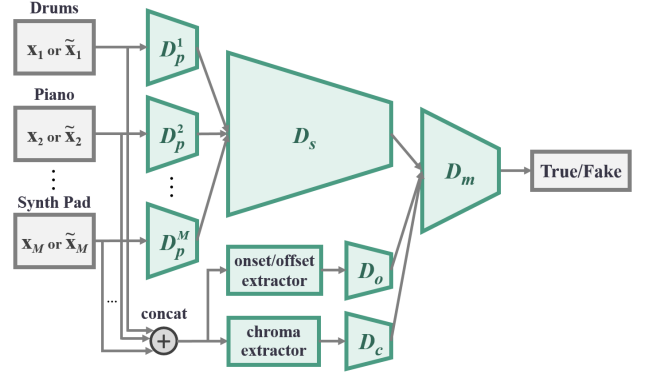


**Figure 5.** The discriminator. It consists of three streams: the main stream (the upper half), the onset/offset stream and the chroma stream.

The values indicate the presence of notes over different time steps. For the time steps, we use symbolic timing.<sup>5</sup>

### 3.2 Generator

As Figure 3 shows, the generator  $G$  consists of a “s”hared network  $G_s$  followed by  $M$  “p”rivate network  $G_p^i$ ,  $i = 1, \dots, M$ , one for each track. The shared generator  $G_s$  first produces a high-level representation of the output musical segments that is shared by all the tracks. Each private generator  $G_p^i$  then turns such abstraction into the final piano-roll output for the corresponding track. The intuition is that different tracks have their own musical properties (e.g., textures, common-used patterns, playing techniques), while jointly they follow a common, high-level musical idea. The design is slightly different from [9] in that the latter does not include a shared  $G_s$  in early layers.

### 3.3 Refiner

The refiner  $R$  is composed of  $M$  private networks  $R^i$ ,  $i = 1, \dots, M$ , again one for each track. The refiner aims to refine the real-valued outputs of the generator,  $\hat{\mathbf{x}} = G(\mathbf{z})$ , into binary ones,  $\tilde{\mathbf{x}}$ , rather than learning a new mapping from  $G(\mathbf{z})$  to the data space. Hence, we draw inspiration from *residual learning* and propose to construct the refiner with a number of *residual units* [16], as shown in Figure 4.

The output layer of the refiner is made up of either DBNs or SBNs. Let  $\bar{R}$  denote the mapping of the refiner with its output layer removed. Then, for the refiner with DBNs, we have

$$R(G(z)) = u(\sigma(\bar{R}(G(z)))) - v, \quad v \sim U[0, 1], \quad (4)$$

where  $u(\cdot)$  denotes the unit step function. For the refiner with SBNs we have

$$R(G(z)) = u(\sigma(\bar{R}(G(z)))) - 0.5. \quad (5)$$

<sup>5</sup> The time axis of a piano-roll can be either in *absolute timing* or *symbolic timing*. For absolute timing, the actual timing of note onsets and offsets are used, while for symbolic timing, tempo information is removed and each beat has the same length regardless of the tempo.

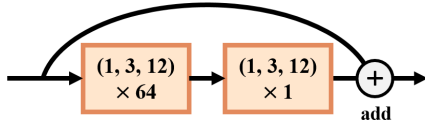


**Figure 6.** Residual unit used in the refiner network. The values denote the kernel size and the number of the output channels of the two convolutional layers.

### 3.4 Discriminator

Similar to the generator, the discriminator  $D$  consists of  $M$  private network  $D_p^i$ ,  $i = 1, \dots, M$ , one for each track, followed by a shared network  $D_s$ , as shown in Figure 5. Each private network  $D_p^i$  first extracts low-level features from the corresponding track of the input piano-roll. Their outputs are concatenated and sent to the shared network  $D_s$  to extract higher-level abstraction shared by all the tracks. The design differs from [9] in that the latter use only one (shared) discriminator to evaluate all the tracks collectively.

As a minor contribution, to help the discriminator extract musically-relevant features, we propose to add to the discriminator two more streams, shown in the lower half of Figure 5. In the first *onset/offset stream*, the differences between adjacent elements in the piano-roll along the time axis are first computed, and then the resulting matrix is summed along the pitch axis, which is finally fed to  $D_o$ .

In the second *chroma stream*, the piano-roll is viewed as a sequence of one-beat-long frames. A chroma vector is then computed for each frame and jointly form a matrix, which is then be fed to  $D_c$ . Note that all the operations involved in computing the chroma and onset/offset features are differentiable, and thereby we can still train the whole network by backpropagation.

Finally, the intra-bar features extracted from the three streams are fed to  $D_m$  to extract inter-bar features and to make the final prediction.

### 3.5 Training

We propose to train the model in a two-stage manner:  $G$  and  $D$  are pretrained in the first stage;  $R$  is then trained along with  $D$  (fixing  $G$ ) in the second stage. Other training strategies are discussed and compared in Section 4.5.

## 4. ANALYSIS OF THE GENERATED RESULTS

### 4.1 Training Data

We use the Lakh Pianoroll Dataset (LPD) [9],<sup>6</sup> which contains 174,154 multi-track piano-rolls derived from the MIDI files in the Lakh MIDI Dataset (LMD) [23].<sup>7</sup> A cleansed subset (*LPD-cleansed*) is also available, which contains 21,425 multi-track piano-rolls that are in 4/4 time and have been matched to distinct entries in Million Song

Dataset (MSD) [4]. We consider only songs with an *alternative* tag in *LPD-cleansed* and randomly pick six four-bar phrases from each song, leading to the final training set of 13,746 phrases from 2,291 songs.

We set the temporal resolution to 24 time steps per beat to cover common temporal patterns such as triplets and 32th notes. An additional one-time-step-long pause is added between two consecutive (i.e. without a pause) notes of the same pitch to distinguish them from one single note. The note pitch has 84 possibilities, from C1 to B7.

We categorize all instruments into drums and sixteen instrument families according to the specification of General MIDI Level 1.<sup>8</sup> We discard the less popular instrument families in LPD and use the following eight tracks: *Drums, Piano, Guitar, Bass, Ensemble, Reed, Synth Lead* and *Synth Pad*. Hence, the size of the target output tensor is  $4$  (bar)  $\times$   $96$  (time step)  $\times$   $84$  (pitch)  $\times$   $8$  (track).

### 4.2 Implementation Details

The size of the input random vector is 128. As shown in Figure 6,  $R$  has two pre-activation residual units [16]. Each convolutional layer is pre-activated by ReLUs, which is preceded by a batch normalization layer. See Table 3 for the network architectures of  $G$  and  $D$ . For all the experiments, we use the Adam optimizer [19], as suggested by [13], with hyperparameters  $\alpha = 0.002$ ,  $\beta_1 = 0.5$ ,  $\beta_2 = 0.9$  and  $\epsilon = 10^{-8}$ . We apply the *slope annealing trick* [8] to networks with DBNs and SBNs, where the slope in ST estimator is multiplied by 1.1 after each epoch. The batch size is 16 except for the pretraining phase in the two-stage training setting, where the batch size is 32.

### 4.3 Evaluation Metrics

We evaluate our results quantitatively in terms of the following metrics proposed in our previous work [9]:

- **Qualified note rate (QN)** computes the ratio of the number of the qualified notes (notes no shorter than three time steps, i.e., a 32th note) to the total number of notes. Low QN implies overly fragmented music.
- **Polyphonicity (PP)** is defined as the ratio of the number of time steps where more than two pitches are played to the total number of time steps.
- **Tonal distance (TD)** measures the distance between the chroma features (one for each beat) of a pair of tracks in the tonal space proposed in [15].

### 4.4 Comparison of Binarization Strategies

We compare the proposed model with two common test-time binarization strategies: *Bernoulli sampling* (BS) and *hard thresholding* (HT). Some qualitative results are provided in Figures 7 and 8. Moreover, we present in Table 1 a quantitative comparison among them.

Both qualitative and quantitative results show that the two test-time binarization strategies can lead to overly-fragmented piano-rolls (see the “pretrained” ones). The

<sup>6</sup> <https://salu133445.github.io/lakh-pianoroll-dataset/>

<sup>7</sup> <http://colinraffel.com/projects/lmd/>

<sup>8</sup> <https://www.midi.org/specifications/item/gm-level-1-sound-set>

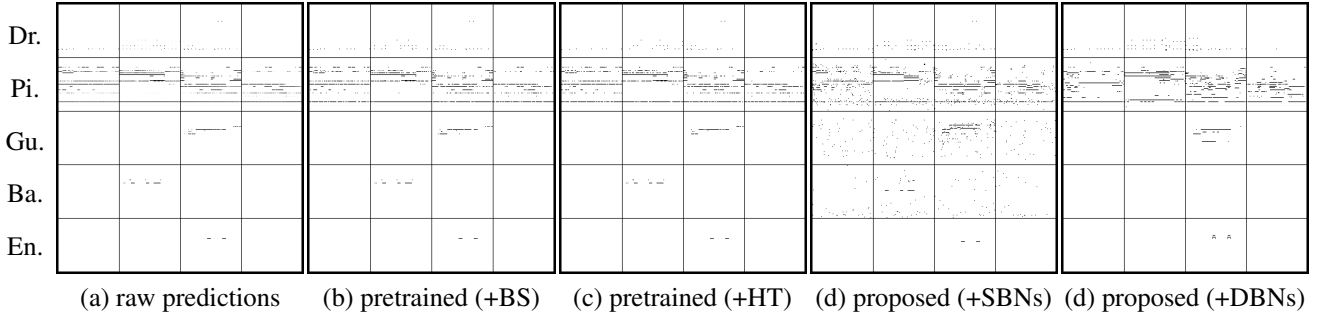


**Figure 7.** Comparison of binarization strategies. (a): the real-valued predictions of the pretrained  $G$ . (b), (c): the results of applying post-processing algorithms directly to the raw predictions. (d), (e): the results of the proposed models, using an additional refiner  $R$  trained in the second stage to binarize the real-valued predictions of  $G$ . Empty tracks are not shown.\*

\*We note that in (d), few noises (33 pixels) occur in the *Reed* and *Synth Lead* tracks.

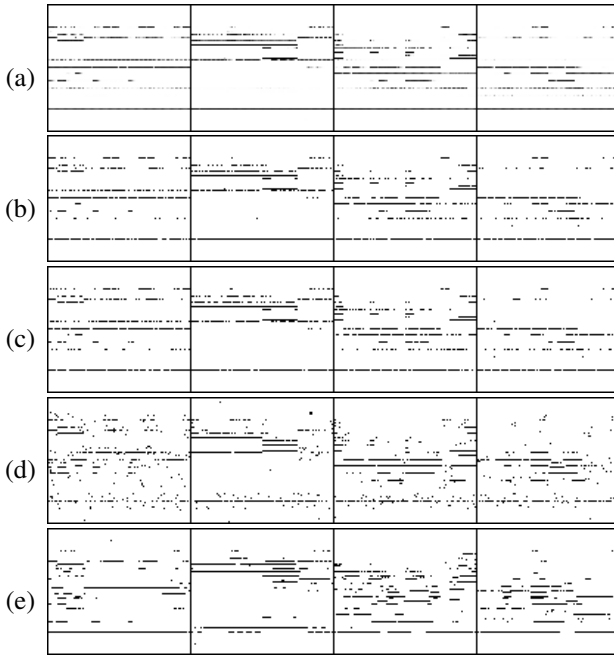


**Figure 8.** Closeup of the piano track in Figure 7.

proposed model with DBNs is able to generate piano-rolls with a relative small number of overly-fragmented notes (a **QN** of 0.78) and to better capture the statistical properties of the training data in terms of **PP**. However, the proposed model with SBNs produces a number of random-noise-like artifacts in the generated piano-rolls, as can be seen in Figure 8, leading to a low **QN** of 0.42, which we attribute to the stochastic nature of SBNs. Moreover, we can also see from Figure 9 that only the proposed model with DBNs keeps improving after the second-stage training starts in terms of **QN** and **PP**.

#### 4.5 Comparison of Training Strategies

We consider two alternative training strategies:

- **joint**: pretrain  $G$  and  $D$  in the first stage, and then train  $G$  and  $R$  (like viewing  $R$  as part of  $G$ ) jointly with  $D$  in the second stage.
- **end-to-end**: train  $G$ ,  $R$  and  $D$  jointly in one stage.

As shown in Table 1, the models with DBNs trained

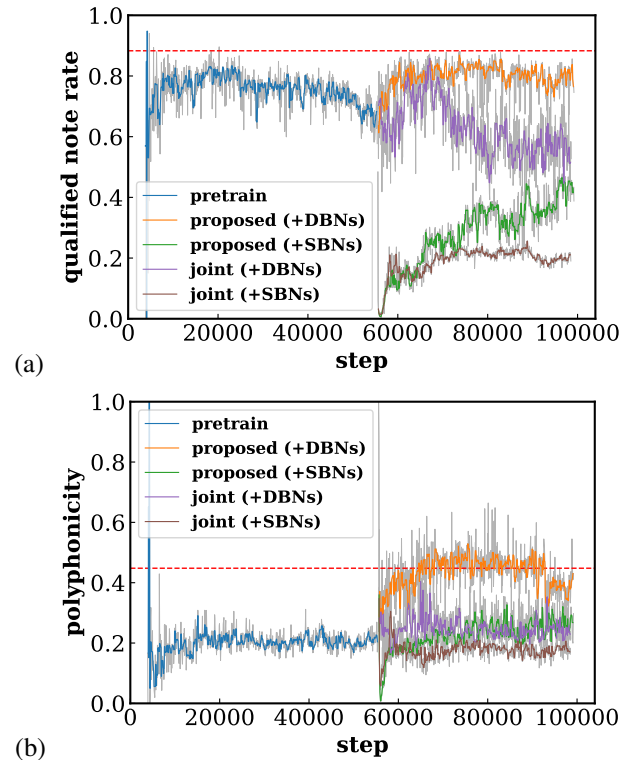


**Figure 9.** (a) Qualified note rate (QN) and (b) polyphonicity (PP) as a function of training steps for different models. The dashed lines indicate the metric values calculated from the training data. (Best viewed in color.)

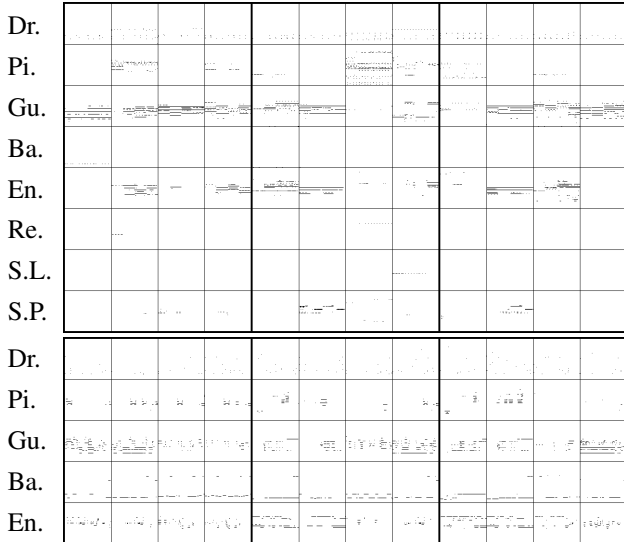
using the *joint* and *end-to-end* training strategies receive lower scores as compared to the *two-stage* training strategy in terms of **QN** and **PP**. We can also see from Figure 9(a) that the model with DBNs trained using the *joint* training strategy starts to degenerate in terms of **QN** at about 10,000 steps after the second-stage training begins.

Figure 10 shows some qualitative results for the *end-to-end* training strategy. We see that the model can learn the proper pitch ranges for different tracks. We also observe some chord-like patterns shown in the generated piano-rolls. Although the generated results appear preliminary, to our best knowledge this represents the first attempt to generate such high dimensional data with SBNs from scratch.

	training data	pretrained		proposed		joint		end-to-end		ablated		baseline	
		BS	HT	SBNs	DBNs	SBNs	DBNs	SBNs	DBNs	BS	HT	BS	HT
<b>QN</b>	0.88	<b>0.67</b>	<b>0.72</b>	0.42	<b>0.78</b>	0.18	0.55	<b>0.67</b>	0.28	0.61	0.64	0.35	0.37
<b>PP</b>	0.48	0.20	0.22	<b>0.26</b>	<b>0.45</b>	0.19	0.19	0.16	<b>0.29</b>	0.19	0.20	0.14	0.14
<b>TD</b>	0.96	<b>0.98</b>	1.00	<b>0.99</b>	0.87	<b>0.95</b>	1.00	1.40	1.10	1.00	1.00	1.30	1.40

(Underlined and bold values indicate the closest and the top 3 closest values, respectively, to the values for the training data for the three metrics.)

**Table 1.** Evaluation results for different models.



**Figure 10.** Example generated piano-rolls of the end-to-end models with (top) DBNs and (bottom) SBNs. Empty tracks are not shown.

#### 4.6 Effects of the Shared/private and Multi-stream Design of the Discriminator

To examine the shared/private and multi-stream design of the discriminator, we compare the proposed model with an *ablated* version that removes the onset/offset and chroma streams. We also include a *baseline* model that uses only a shared discriminator without the shared/private design, which is also the architecture adopted in our previous work [9].<sup>9</sup> Note that the comparison is done by applying the two test-time binarization strategies (i.e. BS and HT) to the first-stage pretrained models.

As shown in Table 1, the proposed design (see the “pre-trained” ones) outperforms the ablated and baseline models in all three metrics. A lower **QN** for the proposed design as compared to the ablated version suggests that the onset/offset stream can alleviate the overly-fragmented note problem. A lower **TD** for both the proposed and the ablated design as compared to the baseline model also indicates that the shared/private design can better capture the intertrack harmonicity. Moreover, we present in Figure 11 the **QN** for the three models along the training process. We can see that the proposed and the ablated model learn faster and better than the baseline model in terms of **QN**.

<sup>9</sup> The number of parameters for the proposed, ablated and baseline model is 3.7M, 3.4M and 4.6M, respectively.

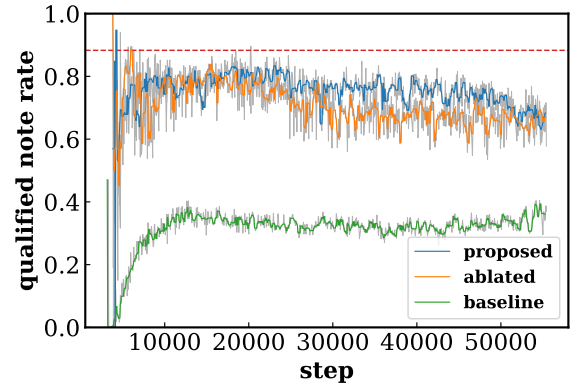


**Figure 11.** Qualified note rate (QN) as a function of training steps for different models. The dashed line indicates the average QN of the training data. (Best viewed in color.)

	with SBNs	with DBNs
completeness*	0.19	<b>0.81</b>
harmonicity	0.44	<b>0.56</b>
rhythmicity	<b>0.56</b>	0.44
overall rating	0.16	<b>0.84</b>

\*We asked, “Are there many overly-fragmented notes?”

**Table 2.** Result of user study, averaged over 20 subjects.

## 5. USER STUDY

Finally, we conduct a user study involving 20 participants recruited from the Internet. In each trial, each subject is asked to compare two pieces of four-bar music generated from scratch by the proposed model using SBNs and DBNs, and vote for the better one in four measures. There are five trials in total per subject. We report in Table 2 the ratio of votes each model receives. The results show a preference to DBNs for the proposed model.

## 6. CONCLUSION

We have presented a novel convolutional GAN-based model for generating binary-valued piano-rolls by using binary neurons at the output layer of the generator. We trained the model on an eight-track piano-roll dataset. Analysis showed that the generated results of our model with deterministic binary neurons features fewer overly-fragmented notes as compared with existing methods. In future work, we plan to add recurrent layers for better temporal model, and to further explore the end-to-end models.

## 7. REFERENCES

- [1] Binary stochastic neurons in tensorflow, 2016. Blog post on R2RT blog. [Online] <https://r2rt.com/binary-stochastic-neurons-in-tensorflow.html>.
- [2] Martin Arjovsky, Soumith Chintala, and Léon Bottou. Wasserstein GAN. In *Proc. ICML*, 2017.
- [3] Yoshua Bengio, Nicholas Léonard, and Aaron C. Courville. Estimating or propagating gradients through stochastic neurons for conditional computation. *arXiv preprint arXiv:1308.3432*, 2013.
- [4] Thierry Bertin-Mahieux, Daniel P.W. Ellis, Brian Whitman, and Paul Lamere. The Million Song Dataset. In *Proc. ISMIR*, 2011.
- [5] Nicolas Boulanger-Lewandowski, Yoshua Bengio, and Pascal Vincent. Modeling temporal dependencies in high-dimensional sequences: Application to polyphonic music generation and transcription. In *Proc. ICML*, 2012.
- [6] Jean-Pierre Briot, Gaëtan Hadjeres, and François Pachet. Deep learning techniques for music generation: A survey. *arXiv preprint arXiv:1709.01620*, 2017.
- [7] Hang Chu, Raquel Urtasun, and Sanja Fidler. Song from PI: A musically plausible network for pop music generation. In *Proc. ICLR, Workshop Track*, 2017.
- [8] Junyoung Chung, Sungjin Ahn, and Yoshua Bengio. Hierarchical multiscale recurrent neural networks. In *Proc. ICLR*, 2017.
- [9] Hao-Wen Dong, Wen-Yi Hsiao, Li-Chia Yang, and Yi-Hsuan Yang. MuseGAN: Symbolic-domain music generation and accompaniment with multi-track sequential generative adversarial networks. In *Proc. AAAI*, 2018.
- [10] Douglas Eck and Jürgen Schmidhuber. Finding temporal structure in music: blues improvisation with LSTM recurrent networks. In *Proc. IEEE Workshop on Neural Networks for Signal Processing*, 2002.
- [11] Ian J. Goodfellow et al. Generative adversarial nets. In *Proc. NIPS*, 2014.
- [12] Ian J. Goodfellow, Jonathon Shlens, and Christian Szegedy. Explaining and harnessing adversarial examples. In *Proc. ICLR*, 2015.
- [13] Ishaan Gulrajani, Faruk Ahmed, Martin Arjovsky, Vincent Dumoulin, and Aaron Courville. Improved training of Wasserstein GANs. In *Proc. NIPS*, 2017.
- [14] Gaëtan Hadjeres, François Pachet, and Frank Nielsen. DeepBach: A steerable model for Bach chorales generation. In *Proc. ICML*, 2017.
- [15] Christopher Harte, Mark Sandler, and Martin Gasser. Detecting harmonic change in musical audio. In *Proc. ACM MM Workshop on Audio and Music Computing Multimedia*, 2006.
- [16] Kaiming He, Xiangyu Zhang, Shaoqing Ren, and Jian Sun. Identity mappings in deep residual networks. In *Proc. ECCV*, 2016.
- [17] Geoffrey Hinton. Neural networks for machine learning - using noise as a regularizer (lecture 9c), 2012. Coursera, video lectures. [Online] <https://www.youtube.com/watch?v=LN0xtUuJsEI>.
- [18] Cheng-Zhi Anna Huang, Tim Cooijmans, Adam Roberts, Aaron Courville, and Douglas Eck. Counterpoint by convolution. In *Proc. ISMIR*, 2017.
- [19] Diederik P. Kingma and Jimmy Ba. Adam: A method for stochastic optimization. *arXiv preprint arXiv:1412.6980*, 2014.
- [20] Stefan Lattner, Maarten Grachten, and Gerhard Widmer. Imposing higher-level structure in polyphonic music generation using convolutional restricted boltzmann machines and constraints. *arXiv preprint arXiv:1612.04742*, 2016.
- [21] Hyungui Lim, Seungyeon Rhyu, and Kyogu Lee. Chord generation from symbolic melody using BLSTM networks. In *Proc. ISMIR*, 2017.
- [22] Olof Mogren. C-RNN-GAN: Continuous recurrent neural networks with adversarial training. In *NIPS Workshop on Constructive Machine Learning Workshop*, 2016.
- [23] Colin Raffel. *Learning-Based Methods for Comparing Sequences, with Applications to Audio-to-MIDI Alignment and Matching*. PhD thesis, Columbia University, 2016.
- [24] Adam Roberts, Jesse Engel, Colin Raffel, Curtis Hawthorne, and Douglas Eck. A hierarchical latent vector model for learning long-term structure in music. *arXiv preprint arXiv:1803.05428*, 2018.
- [25] Bob L. Sturm, João Felipe Santos, Oded Ben-Tal, and Iryna Korshunova. Music transcription modelling and composition using deep learning. In *Proc. Conf. Computer Simulation of Musical Creativity*, 2016.
- [26] Christian Szegedy et al. Intriguing properties of neural networks. *arXiv preprint arXiv:1312.6199*, 2013.
- [27] Li-Chia Yang, Szu-Yu Chou, and Yi-Hsuan Yang. MidiNet: A convolutional generative adversarial network for symbolic-domain music generation. In *Proc. ISMIR*, 2017.
- [28] Lantao Yu, Weinan Zhang, Jun Wang, and Yong Yu. SeqGAN: Sequence generative adversarial nets with policy gradient. In *Proc. AAAI*, 2017.

<b>Input:</b> $\mathbb{R}^{128}$						
<i>dense</i>	1536					
reshape to $(3, 1, 1) \times 512$ channels						
<i>transconv</i>	256	$2 \times 1 \times 1$	$(1, 1, 1)$			
<i>transconv</i>	128	$1 \times 4 \times 1$	$(1, 4, 1)$			
<i>transconv</i>	128	$1 \times 1 \times 3$	$(1, 1, 3)$			
<i>transconv</i>	64	$1 \times 4 \times 1$	$(1, 4, 1)$			
<i>transconv</i>	64	$1 \times 1 \times 3$	$(1, 1, 2)$			
		substream I		substream II		
<i>transconv</i>	64	$1 \times 1 \times 12$	$(1, 1, 12)$	64	$1 \times 6 \times 1$	$(1, 6, 1)$
<i>transconv</i>	32	$1 \times 6 \times 1$	$(1, 6, 1)$	32	$1 \times 1 \times 12$	$(1, 1, 12)$
						$\dots \times 8$
concatenate along channel axis						
<i>transconv</i>	1	$1 \times 1 \times 1$	$(1, 1, 1)$			
stack along track axis						
<b>Output:</b> $\mathbb{R}^{4 \times 96 \times 84 \times 8}$						

(a) generator  $G$ 

<b>Input:</b> $\mathbb{R}^{4 \times 96 \times 84 \times 8}$						
split along track axis						
		substream I		substream II		
<i>conv</i>	32	$1 \times 1 \times 12$	$(1, 1, 12)$	32	$1 \times 6 \times 1$	$(1, 6, 1)$
<i>conv</i>	64	$1 \times 6 \times 1$	$(1, 6, 1)$	64	$1 \times 1 \times 12$	$(1, 1, 12)$
						$\dots \times 8$
concatenate along channel axis						
<i>conv</i>	64	$1 \times 1 \times 1$	$(1, 1, 1)$			
concatenate along channel axis						
<i>conv</i>	128	$1 \times 4 \times 3$	$(1, 4, 2)$			
<i>conv</i>	256	$1 \times 4 \times 3$	$(1, 4, 3)$			
concatenate along channel axis						
<i>conv</i>	512	$2 \times 1 \times 1$	$(1, 1, 1)$			
<i>dense</i>	1536					
<i>dense</i>	1					
<b>Output:</b> $\mathbb{R}$						

(b) discriminator  $D$ 

<b>Input:</b> $\mathbb{R}^{4 \times 96 \times 1 \times 8}$			
<i>conv</i>	32	$1 \times 6 \times 1$	$(1, 6, 1)$
<i>conv</i>	64	$1 \times 4 \times 1$	$(1, 4, 1)$
<i>conv</i>	128	$1 \times 4 \times 1$	$(1, 4, 1)$
<b>Output:</b> $\mathbb{R}^{4 \times 1 \times 1} \times 128$ channels			

(c) onset/offset feature extractor  $D_o$ 

<b>Input:</b> $\mathbb{R}^{4 \times 4 \times 12 \times 8}$			
<i>conv</i>	64	$1 \times 1 \times 12$	$(1, 1, 12)$
<i>conv</i>	128	$1 \times 4 \times 1$	$(1, 4, 1)$
<b>Output:</b> $\mathbb{R}^{4 \times 1 \times 1} \times 128$ channels			

(d) chroma feature extractor  $D_c$ 

<b>Input:</b> $\mathbb{R}^{4 \times 96 \times 84 \times 8}$			
<i>conv</i>	128	$1 \times 1 \times 12$	$(1, 1, 12)$
<i>conv</i>	128	$1 \times 1 \times 3$	$(1, 1, 2)$
<i>conv</i>	256	$1 \times 6 \times 1$	$(1, 6, 1)$
<i>conv</i>	256	$1 \times 4 \times 1$	$(1, 4, 1)$
<i>conv</i>	512	$1 \times 1 \times 3$	$(1, 1, 3)$
<i>conv</i>	512	$1 \times 4 \times 1$	$(1, 4, 1)$
<i>conv</i>	1024	$2 \times 1 \times 1$	$(1, 1, 1)$
reshape to (3072,)			
<i>dense</i>	1		
<b>Output:</b> $\mathbb{R}$			

(e) baseline discriminator

**Table 3.** Network architectures for the (a) generator  $G$ , (b) discriminator  $D$ , (c) onset/offset feature extractor  $D_o$ , (d) chroma feature extractor  $D_c$  and (e) baseline discriminator. For convolutional (*conv*) and transposed convolutional (*transconv*) layers, the values represent (from left to right): the number of filters, kernel size and strides. For dense layers (*dense*), the value represents the number of nodes. Each transposed convolutional layer in  $G$  is followed by a batch normalization layer and then activated by ReLUs except for the last layer, which is activated by sigmoid functions. Convolutional layers in  $D$  are activated by LeakyReLUs except for the last layer, which has no activation function.